SHIP ROLLING MOTION SUBJECTED TO COLORED NOISE EXCITATION

A Thesis

by

ARADA JAMNONGPIPATKUL

Submitted to the Office of Graduate Studies of
Texas A&M University
in partial fulfillment of the requirements for the degree of

MASTER OF SCIENCE

December 2010

Major Subject: Ocean Engineering

SHIP ROLLING MOTION SUBJECTED TO COLORED NOISE EXCITATION

A Thesis

by

ARADA JAMNONGPIPATKUL

Submitted to the Office of Graduate Studies of
Texas A&M University
in partial fulfillment of the requirements for the degree of

MASTER OF SCIENCE

Approved by:

Chair of Committee,	Jeffrey Falzarano
Committee Members,	Moo-Hyun Kim
	Tamás Kalmár-Nagy
Head of Department,	John Niedzwecki

December 2010

Major Subject: Ocean Engineering

ABSTRACT

Ship Rolling Motion Subjected to Colored Noise Excitation. (December 2010)

Arada Jamnongpipatkul, B.Eng., Chulalongkorn University

Chair of Advisory Committee: Dr. Jeffrey Falzarano

In this research the stochastic nonlinear dynamic behaviors and probability density function of ship rolling are studied by nonlinear dynamic method and probability theory. The probability density function of rolling response is evaluated through solving the stochastic differential equations by using path integral method based on Gauss-Legendre interpolation scheme. The time-dependent probability of ship rolling restricted within the safe domain is provided and capsizing is investigated in the probability's view.

The random differential equation of ships' rolling motion is established considering the nonlinear damping, nonlinear restoring moment, the white noise wave excitation, and the colored noise wave excitation. As an example, an ocean survey vessel T-AGOS is considered to sail in the seas of Pierson-Moskowitz wave spectrum.

It is found that the probability decreases as time progresses and it decreases much more quickly for the high intensity of the noise. The ship will finally leave the safe domain and capsize in the probability's view. It is also shown the similarity of probability density contours between the case of white noise wave excitation and the case of colored noise wave excitation.

ACKNOWLEDGEMENTS

I would like to thank my committee chair, Dr. Jeffrey Falzarano, and my committee members, Dr. Moo-Hyun Kim, and Dr. Tamás Kalmár-Nagy, for their guidance and kindest support throughout the course of this research. Thanks also go to the department faculty, staff, all my research group members, and friends for making my time at Texas A&M University a great experience.

Finally, thanks to my mother, father, and sister for their consistent encouragement.

TABLE OF CONTENTS

LIST OF FIGURES

FIGURE Page

CHAPTER I

INTRODUCTION

The purpose of this project is to study the qualitative behavior of the ship rolling motion in probability space. We analyze large amplitude vessel motions which may lead to capsizing. Chapters of the project are organized as follows.

Chapter II provides motivation for the current work by describing a few ship stability projects about how they are analyzing similar problems. The ship dynamics aspects of the problem and the simple model for vessel roll dynamics are described in Chapter III. To discover the properties of the systems, the associated stochastic differential equations will be solved numerically to get the joint probability density functions. Chapter IV is a review and examination of the path integration method. The numerical path integration based on the Gauss-Legendre interpolation scheme is derived. The theoretical background of path integral is briefly presented, followed by a general discussion of numerical implementations. This provides a good understanding of how the procedure works. Following the theoretical development of path integration method, numerical examples have been demonstrated to verify the efficiency of computer program. In Chapter V, the procedure proposed in Chapter IV is applied to ship rolling system subjected to the case of white noise and sinusoidal excitations and the case of colored noise. Results from numerical simulations are presented. The project is closed with some conclusions and directions for future work in Chapter VI.

This thesis follows the style of *Journal of Ship Research*.

CHAPTER II

LITERATURE REVIEW

General

Safety against capsizing in heavy sea is one of the major concerns of ship operators and designers. Although the data of ship capsizing is scattered, it was often reported in the media. Recently, CBS.com reported on Feb, 20, 2010, school ship capsized in 15 second in Brazil's Atlantic coast. In fact, many ships still experienced capsizing in the heavy seas even their design satisfied all the stability standards. This is because the existing criteria consider only the ship's static stability, which is based only on the ship's nonlinear restoring moment curve. The criteria were not correspondent with the complex nature of the capsize phenomenon and the large numbers of possible scenarios. Dynamical theories and methods may better explain ship capsizing mechanism since capsizing is a dynamic phenomenon. Consequently, dynamic behaviors of ship have been of interest to many researchers and engineers, particularly in stability of roll motion.

Prior to capsizing, ships will undergo severe roll motion. The motion is believed to be chaotic. Identifying the chaotic motion and its critical condition are important for both predicting ships' capsizing and study the capsize mechanism.

Chaotic Motion

Ship rolling even in a regular sea can exhibit complicated behavior, leading to instability and eventually capsizing. Although pure regular waves do not occur in nature, much work has been done on analyses for vessels subjected to a periodic excitation in a simplified sea state in order for us to understand the mechanism of ship roll motion under the influence of nonlinear stiffness and nonlinear damping. Falzarano et al (1992) analyzed the global stability of ship in regular waves by the use of the Melnikov method

and lobe dynamics to define the critical parameters for onset of chaos that might lead to capsizing and explained the unexpected capsizing in both homoclinic and heteroclinic regions. Ship rolling in homoclinic region is the case of ship oscillation around the loll angle while ship rolling in heteroclinic region represents large amplitude roll motion, which results in ship rolling between positive and negative angles. By using the Melnikov method to identify the chaotic motion and its critical conditions, it is a significant tool for the prediction and study of ship capsizing. The so-called chaotic phenomena appear when the behavior of a deterministic system depends sensitively upon initial conditions and then becomes long-term unpredictable.

However, realistic waves, which affect a ship's safety, are random and irregular. In order to make the models more accurate and gain a better understanding of stability of ship rolling motion, the wave excitation was later treated as regular waves perturbed by random noise. Then the ship may experience stochastic chaotic motion. Some initial research about the effects of noise on chaotic behavior of nonlinear systems has been conducted in ship dynamics and also other engineering fields. Hsieh et al (1994) finished a more realistic work by analyzing a single-degree-of-freedom nonlinear rolling equation in random beam sea. The random Melnikov mean-square criterion was derived and used to calculate the threshold intensity of external force for onset of chaos and determine the chaotic parameter domain. Moreover, they introduced the rate of phase space flux and studied its relation to the probability of capsizing. However, no standard method is set for identifying the chaotic motion of ship in random waves.

Lin & Yim (1995, 2001) and Liqin & Yougang (2007) studied the stochastic chaotic motion of ship under periodic excitation with the disturbance approximated by Gaussian white noise from a probability perspective. The joint probability density function of roll angle and roll angular velocity was calculated by applying the path integral method to solve the stochastic differential equations governing ship rolling motion. Lin and Yim found that the steady-state joint probability density functions can reflect the existing chaotic attractor on the Poincaré section and also the roll response in

the heteroclinic region can be related to the capsizing through the joint probability density functions. To examine the chaotic characteristic of nonlinear roll motion in an unpredictable sea state, one cannot avoid dealing with probabilistic approaches. The shape evolution of the probability density function is another way to investigate the global system behavior.

Gaussian white noise has become an important factor in these studies. The response of a dynamical system, roll angle and roll angular velocity in ship rolling study, under periodic excitation and Gaussian white noise can be modeled as a Markov process whose transition probability density function is governed by a partial differential equation called the Fokker-Planck equation. Solving the Fokker-Planck equation would provide an alternative mean to express the evolution of the probability density function.

Narrow-band Random Wave

To further study a more realistic system, a narrow-band random excitation is introduced and replacing the Gaussian white noise which is widely known as a wide-band random process. Comparatively, the study of dynamical systems subjected to a narrow-band random excitation is also considered important but is still limited. However, this introduction shall be an advantageous proceeding for study in naval architecture and marine engineering since the spectrum of ocean wave has a finite peak and a narrow bandwidth.

Nowadays, there are two different ways that are broadly used for modeling a narrow-band random excitation. One is the so-called bounded noise. The other is called filtered white noise or colored noise.

The bound noise represents a narrow-band process by using a harmonic function with constant amplitude and random frequency and phase. It has finite power and by choosing different parameters its spectrum shape can be fitted into various target

spectrums. This bounded noise should be a good approximate model for the random excitation in engineering field.

Huang et al (2002) studied a single-degree-of-freedom strongly nonlinear system under bounded noise excitation which is represented as generalized harmonics functions. A stochastic averaging method was used to analyze behavior near the resonance condition. It was found that the noise is also able to make the system approach an equilibrium position. Moreover, in the field of naval architecture and marine engineering, Hu et al (2010) illustrated that the power spectral density of ocean wave, such as the widely used Pierson-Moskowitz spectrum, can be described quite well by a bounded noise spectrum especially in the main frequency region, as seen in Figure 1. They used the random Melnikov mean-square criterion to find the threshold of bounded noise amplitude for the onset of chaos.

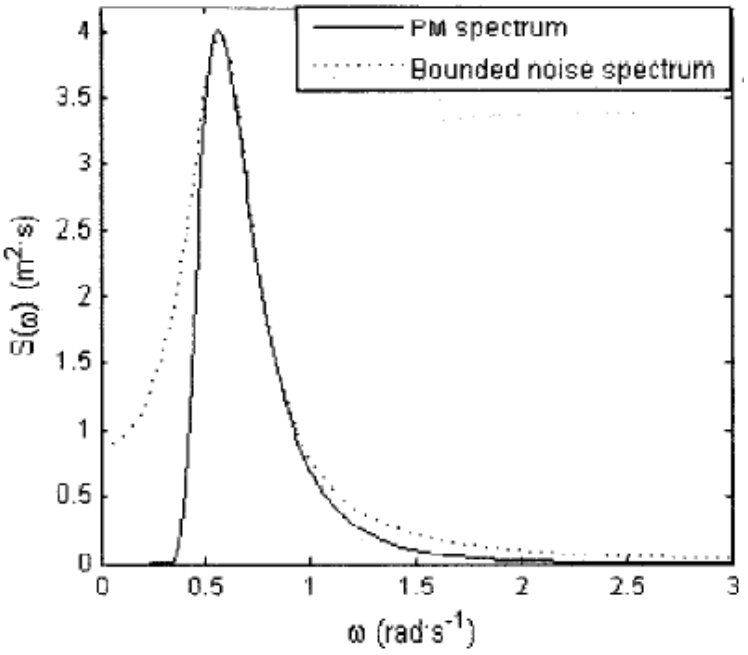

Figure 1. Approximation of the Pierson-Moskowitz spectrum by bounded noise (Hu et al 2010)

Besides bounded noise, creating the so-called colored noise by linearly filtering stationary Gaussian white noise is another means to model a narrow-band random excitation. The response of the filter is then used to drive the nonlinear system. When these filter equations are added to the original equation of motion, the whole system is excited by Gaussian white noise. In this way, the advantage of Markov process still exists. Davies & Nandlall (1986) studied a hardening Duffing oscillator excited by a filtered white noise. The Fokker-Planck-Kolmogorov equation approach was applied through equivalent linearization to construct the phase plane portraits. It is shown that there could be a multivalued response occurring at some frequencies but those values could be reduced to a single one when the bandwidths were increase.

Since it is possible to rewrite the system subjected to colored noise excitation in terms of a Markov process, the Fokker-Planck equation governing the probability density function is obtained. The Fokker-Planck equation has to be solved in order to illustrate the evolution of probability density functions but exact solutions for this equation are available only for linear systems and some first-order nonlinear systems. Due to the difficulties in solving the Fokker-Planck equation for nonlinear systems, some approximate numerical methods subject to different limitations have been proposed for solving nonlinear stochastic differential equations such as the equivalent linearization method (Davies & Nandall 1986), the finite element technique (Xie et al 2007) and the stochastic averaging method (Davies & Liu 1990).

CHAPTER III

PROBLEM DESCRIPTION

Ship Rolling Equation

The problem of ship rolling motion has been approached several times in the past. It is shown that rolling response of the ship exhibits irregular and complicated behaviors, even in the regular sea with moderate excitation amplitude. In this project, an analysis of large amplitude nonlinear ship rolling motion in beam seas subjected to different models of excitation is presented.

Ship rolling motion is a nonlinear phenomenon in nature and generally coupled with other motions, such as sway, pitch and heave. However, if it is the case of a ship at low speed in unidirectional beam waves, it is reasonable to uncouple roll motion from sway motion and provided that the coordinate origin is located at an appropriate 'roll centre' (Roberts & Vasta 2000). Then, at least for the case of beam waves, the dynamics of large amplitude ship rolling can be captured by the single-degree-of-freedom equation of motion for the roll angle ϕ. The nonlinear differential equation of the ship rolling motion was established considering nonlinear damping and nonlinear restoring moment. The governing equation can be expressed as follows for ships in beam wave (Hsieh et al 1994).

$$(I_{44} + A_{44}(\omega))\phi'' + B_{44}(\omega)\phi' + B_{44q}(\omega)\phi'|\phi'| + \Delta GZ(\phi) = F_{sea}(t) \qquad (1)$$

where I_{44} is the moment of inertia of the ships about the roll axis, $A_{44}(\omega)$ is the roll hydrodynamics added mass coefficient, $B_{44}(\omega)$ is the liner viscous damping coefficient, $B_{44q}(\omega)$ is the quadratic viscous damping coefficient, Δ is the vessel displacement, $GZ(\phi)$ is the nonlinear rolling restoring moment, $F_{sea}(t)$ denotes external excitation from waves and a prime denotes a derivative with respect to time t.

Here the nonlinear damping term $\phi'|\phi'|$ is assumed to be of the linear-plus-quadratic type. It has been shown by numerous studies of experimental data that this is a good model (Roberts & Vasta 2000). The method of least squares was applied to fit the term into a cubic polynomial form below.

$$\phi'|\phi'| = a\phi' + b\phi'^3 \tag{2}$$

It is found that when roll angular velocity is in the range of [-1.5, 1.5], a is 0.4689 and b is 0.4859, respectively.

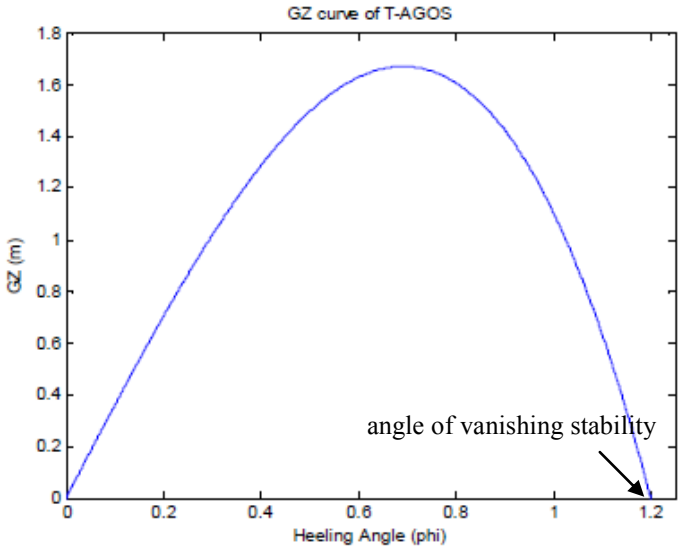

Figure 2. An example of GZ curve (Mulk & Falzarano 1994)

For the restoring moment *GZ(ϕ)*, Figure 2. is the typical GZ curve for this study. It is usually used polynomial fitting the GZ curve. According to the GZ curve in Figure 2., the linear-minus-cubic form chosen as seen in equation (3) for the restoring moment is the simplest model that represents the actual shape of restoring moment versus roll angle curves.

$$GZ(\phi) \approx C_1\phi - C_3\phi^3 \tag{3}$$

where C_1 is the linear restoring moment coefficient and C_3 is the nonlinear coefficient.

The static restoring moment of a ship, which is an important property relating to its stability, is generally of a 'softening' kind such that, as the roll angle increases from zero, it initially increases with ϕ, reaches a maximum value and then falls to zero at some critical angle ϕ^* dubbed the "angle of vanishing stability" as shown in Figure 2. For small angle rolling, the linear restoring term is dominant. The nonlinear term is effective as roll angle increases. When the roll angle exceeds the angle of vanishing stability, GZ becomes negative. This means that the restoring moment becomes negative and results in the loss of stability (McCue & Wu 2008).

Follows from Hsieh et al (1994) by defining a new timescale *t*, equation (1) can be rewritten in the following nondimensional form

$$\ddot{x}(\tau)+\mu\dot{x}(\tau)+\delta\dot{x}^3(\tau)+x(\tau)-\alpha x^3(\tau)=\varepsilon f(\tau) \tag{4}$$

where μ and δ represent , respectively, the dimensionless linear and quadratic viscous damping coefficients, α denotes the strength of the nonlinearity, $\varepsilon f(t)$ is the excitation and differentiation with respect to time t is denoted by an overdot. The non-dimensional terms are defined as

$$x=\phi, \quad \tau=\omega_n t, \quad \omega_n=\sqrt{\frac{\Delta C_1}{I_{44}+A_{44}(\omega)}}, \quad \mu=\frac{B_{44}(\omega)}{\Delta C_1}\omega_n,$$
$$\Omega=\frac{\omega}{\omega_n}, \quad \alpha=\frac{C_3}{C_1}, \quad \delta=\frac{B_{44q}(\omega)}{I_{44}+A_{44}(\omega)}, \quad \varepsilon f(t)=\frac{F_{sea}}{\Delta C_1}$$

Wave Excitation as Colored Noise

In this section, the excitation term on the right-hand-side of equations (1) and (4) will be defined. There are several ways to model excitation arising from beam seas. For example, in the early study, researchers used periodic beam sea as a simplified sea state, shown below, and analyzed the system in detail.

$$(I_{44}(\omega)+A_{44}(\omega))\phi''+B_{44}(\omega)\phi'+B_{44q}(\omega)\phi'|\phi'|+\Delta GZ(\phi)=F\cos(\omega t+\varepsilon_4) \tag{5}$$

where F is the amplitude of the external force due to induced wave with frequency ω and phase angle ε_4 with respect to a wave crest amidships.

The equation (5) was analyzed in detail by many researchers in the past. The studies found that ship rolling motion in regular waves can exhibit the nonlinear phenomena of amplitude jumping, superharmonic and subharmonic response, symmetry breaking, period doubling and chaotic motion. To complement these deterministic studies, it is important to recognize the random nature of ocean waves and include this nature into the analysis by modeling the wave excitation as stochastic processes.

A more realistic work is to use random excitation in the single-degree-of-freedom roll equation. The simplest model is to treat the wave excitation as perturbed regular waves with the disturbance approximated by Gaussian white noise.

$$(I_{44}(\omega) + A_{44}(\omega))\phi'' + B_{44}(\omega)\phi' + B_{44q}(\omega)\phi'|\phi'| + \Delta GZ(\phi) = F\cos(\omega t) + \sqrt{D}N(t) \qquad (6)$$

where $\sqrt{D}N(t)$ is the white noise with intensity of D and $N(t) = dW(t)/dt$, where $W(t)$ is a standard Wiener process.

The behavior of the ship roll motion under combined sinusoidal and Gaussian white noise excitation constitutes a Markov vector process whose transition probability density function is governed by the Fokker-Planck equation. The utilization of these two concepts will be discussed in detail later.

However, for only a special condition, the wave excitation is treated as white noise just to simplify the computation. In real ship evaluation, the realistic wave such as the Pierson-Moskowitz spectrum, given in terms of wave amplitude spectrum $S_{\eta\eta}(\omega)$, should be adopted. The Pierson-Moskowitz spectrum is given by:

$$S_{\eta\eta}(\omega) = \frac{A}{\omega^5}\exp\left(-\frac{B}{\omega^4}\right) \qquad (7)$$

with $A = 8.1\times10^{-3} g^2$ and $B = \dfrac{3.11}{h_{1/3}^2}$ expressed in term of the significant wave height $h_{1/3}$.

For the spectral density function for the excitation, $S_{ff}(\omega)$, it is obtained through the expression:

$$S_{ff}(\omega) = \left|F_{roll}(\omega)\right|^2 S_{\eta\eta}(\omega) \tag{8}$$

where an equivalent single degree of freedom roll moment about a frequency dependent roll centre, $F_{roll}(\omega)$, was formed from the complex, frequency dependent, linear roll and sway exciting moment and force respectively. It is based upon pressures due to waves with small slopes acting on a fixed vessel in the mean (upright) position. This transforms the wave amplitudes into effective moments acting on the vessel. Figure 3. shows the roll moment per unit wave amplitude used in this example.

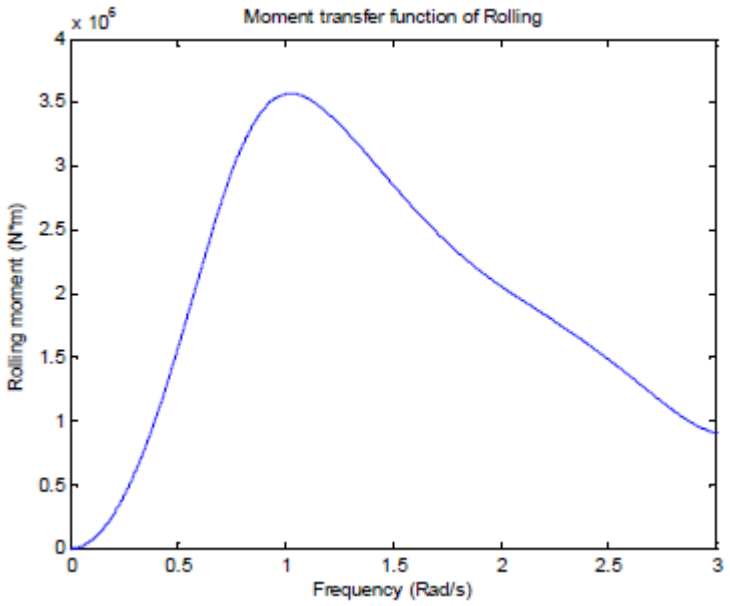

Figure 3. Roll moment per unit wave amplitude (F_{roll}) (Su [2010])

The wave excitation *f(t)* now is irregular and is described by a random process which is assumed stationary, ergodic, zero mean Gaussian and described by a given spectrum. This process can be produced either by the sum of a set of harmonic wave

excitation moment or by the mean of colored noise. A sum of cosine functions is a convenient one to approximate the process stated above. Equation (9) has been used to model the excitation *f* in equation (4). An input signal corresponding to the Pierson-Moskowitz spectrum is obtained in the discretized form.

$$f(t) = \sum_{j=1}^{N} \gamma_j \cos(\omega_j t + \psi_j) \tag{9}$$

when selecting N equally spaced frequencies ω_j in the range of upper and lower frequency bounds $[\omega_L, \omega_U]$ and using cosine amplitudes for each frequency weighted according to $\gamma_j = \sqrt{(2S_{\eta\eta}(\omega_j)\Delta_N}$ where Δ_N is the width of the frequency intervals and finally selecting a set of phases ψ_j for the harmonic components. Different realizations for the input are achieved by selecting different values for these phases. Figure 4. shows typical time history of the excitation.

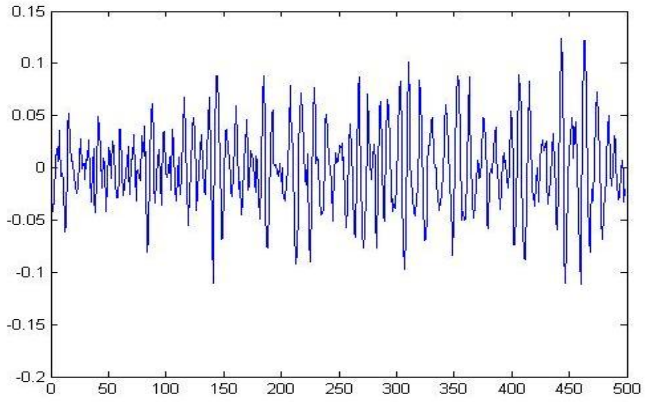

Figure 4. Time history of excitation *f(t)*

However, the main focus in this project is to consider the excitation process obtained by means of linear filter acting on white noise. In order to model a narrow-band random excitation using the colored noise concept, stochastic differential equations are developed and defined as shaping filters. These filters are capable of reproducing known spectrum as shown below. Figure 5 shows the comparison of the exact Pierson-

Moskowitz spectrum and the approximation by various types of filtered white noise excitations.

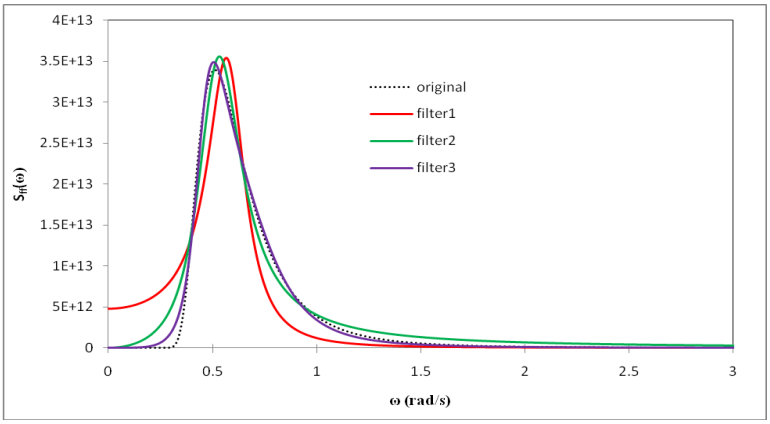

Figure 5. Approximation of the Pierson-Moskowitz by filter equations (Su 2010)

From Figure 5., it is seen that the approximation by filter 1 is reasonable in terms of peak height and band width but there is a non-zero value at zero frequency. Besides, it distributes too much energy in the low frequency range, which usually is a zone where the transfer function to ship roll moment is non-negligible. The approximation by filter 2 is acceptable while the approximation by filter 3 is excellent in all aspects. The stochastic differential equations describe filter 1, filter 2 and filter 3 are equation (10), equation (11) and equation (12), respectively (Francescutto & Naito 2004).

$$F''(t) + c_1 F'(t) + k_1^2 F(t) = \beta_1 N(t) \tag{10}$$

$$F''(t) + c_1 F'(t) + k_1^2 F(t) = \beta_1 N'(t) \tag{11}$$

$$F'''(t) + \lambda_3 F'''(t) + \lambda_2 F''(t) + \lambda_1 F'(t) + \lambda_0 F(t) = \beta_1 N''(t) \tag{12}$$

where $N(t)$ is a unit Gaussian white noise with mean zero $E[N(t)] = 0$ and delta correlation $E[N(t)N(t+\tau)] = \delta(\tau)$ where $\delta(\cdot)$ denotes Dirac's delta function. Other parameters defining the filters have been computed by a standard least-squares method

to fit the known spectrum. These relevant parameters are used to adjust the bandwidth and other important characteristics. When a filter acts on white noise, it produces a random process whose spectrum is given by the function S_i. Each of them corresponds to a linear differential equation translating the effect of the filter transfer function on the white noise process *N(t)*. Equations (13) – (15) are spectrum expressions corresponding to filter equations (10) – (12), respectively (Francescutto & Naito 2004).

$$S_1(\omega) = \frac{\beta_1^2}{[(\omega^2 - k_1^2)^2 + (c_1\omega)^2]} \tag{13}$$

$$S_2(\omega) = \frac{\beta_1^2\omega^2}{[(\omega^2 - k_1^2)^2 + (c_1\omega)^2]} \tag{14}$$

$$S_3(\omega) = \frac{\beta_1^2\omega^4}{[(\omega^2 - k_1^2)^2 + (c_1\omega)^2]\cdot[(\omega^2 - k_2^2)^2 + (c_2\omega)^2]} \tag{15}$$

with $\gamma_1 = (c_1 + c_2)$, $\gamma_2 = (k_1^2 + k_2^2 + c_1c_2)$, $\gamma_3 = (c_1k_2^2 + c_2k_1^2)$, $\gamma_4 = k_1^2k_2^2$ for filter 3.

In this project, a solution of equation (1) for ship rolling in a stochastic beam sea by using filter 2 is developed. Three factors, i.e, random excitation, nonlinear stiffness and nonlinear damping, will form the basis of the nonlinear stochastic model developed in this project.

Markov Process and Fokker-Planck Equation

Consider the following ship rolling equation of motion driven by colored noise process described by

$$\ddot{x}(t) + \mu\dot{x}(t) + \delta\dot{x}^3(t) + x(t) - \alpha x^3(t) = \varepsilon f(t) \tag{16}$$

where ε, δ_1, δ_2, α are constants. The external excitation process *f(t)* of equation (16) is assumed as a colored noise obtained by filtering stationary Gaussian white noise *N*, which satisfies

$$\ddot{f}(t) + c_1 \dot{f}(t) + k_1^2 f(t) = \beta_1 \dot{N}(t) \tag{17}$$

where c_1, k_1 and β_1 are positive constants and $E[N(t)] = 0$ and $E[N(t)N(t+\tau)] = \delta(\tau)$.

Writing equations (16) and (17) in the first-order form as

$$\begin{aligned}
\dot{x}_1(t) &= x_2(t) \\
\dot{x}_2(t) &= -\mu x_2(t) - \delta x_2^3(t) - x_1(t) + \alpha x_1^3(t) + \varepsilon x_3(t) \\
\dot{x}_3(t) &= x_4(t) + \beta_1 N(t) \\
\dot{x}_4(t) &= -c_1 x_4(t) - k_1^2 x_3(t)
\end{aligned} \tag{18}$$

Now in four-dimensional space, the response process of equation (18) is a Markov process. Any random process is called Markov when the probability density function of the process in the future does not depend on how the process arrived at the given state. Hence Markov property is a generalized causality principle and a basic assumption that is made in the study of stochastic dynamical systems. The concept of the Markov operator has been applied in the classical nonlinear random vibration analysis.

The Markov process is governed by the following stochastic Itô equation (Lin et al 1997):

$$d\vec{X}(t) = \vec{f}(\vec{X}, t)dt + \vec{g}(\vec{X}, t)d\vec{W}(t) \tag{19}$$

where $\vec{X}(t)$ is an n-dimensional state vector, $\vec{f}$ is an n-dimensional vector function defined as drift coefficient, $\vec{g}$ is an $n \times m$ matrix function defined as the diffusion coefficient, and $\vec{W}(t)$ is an m-dimensional Wiener vector process, with $E[d\vec{W}(t)] = \vec{0}$ and $E[d\vec{W}(t)d\vec{W}^T(t)] = \vec{I}dt$, and where $\vec{I}$ is an $m \times m$ identity matrix. For the specific ship rolling system in this project, we have

$$\vec{X}(t)=\begin{Bmatrix}x_1\\x_2\\x_3\\x_4\end{Bmatrix},\qquad \vec{f}(\vec{X},t)=\begin{Bmatrix}x_2\\-\mu x_2-\delta x_2^3-x_1+\alpha x_1^3+\varepsilon x_3\\x_4\\-c_1x_4-k_1^2x_3\end{Bmatrix},\qquad \vec{g}(\vec{X},t)=\begin{Bmatrix}0\\0\\\beta_1\\0\end{Bmatrix} \tag{20}$$

In order to solve the ship rolling problem dealing with nonlinear systems driven by stochastic processes, several methods have been used, including the use of statistical linearization, perturbation and functional series, the Fokker-Planck equation, non-Gaussian moment closure, and the use of Melnikov functions. Of these approaches, the use of the Fokker-Planck equation is one of the most attractive approaches since it enables the probability density function of the response to be determined.

When the response of a dynamical system subjected to Gaussian white noise excitation is a Markov process, the transition probability density function of the response satisfies a deterministic parabolic partial differential equation called the Fokker-Planck equation. The associated Fokker-Planck equation governing the evolution of the probability density function of the roll motion is derived from Itô stochastic differential equation as follows

$$\frac{\partial q(\vec{x},t\mid\vec{x}^{(0)},t_0)}{\partial t}=-\frac{\partial}{\partial x_i}[f_i(\vec{x},t)q(\vec{x},t\mid\vec{x}^{(0)},t_0)]+\frac{1}{2}\frac{\partial^2}{\partial x_i\partial x_j}[b_{ij}(\vec{x},t)q(\vec{x},t\mid\vec{x}^{(0)},t_0)] \tag{21}$$

where $\vec{x}$ is the state vector of $\vec{X}(t)$, f_i are components of $\vec{f}$, b_{ij} are elements of matrix $\vec{b}=\vec{g}\vec{g}^T$, and the symbol $\mid\vec{x}^{(0)},t_0$ denotes the given condition $\vec{X}(t_0)=\vec{x}^{(0)}$, $t\le t_0$. Obviously, the Fokker-Planck equation for this project becomes a four-dimensional one. Solving this equation would provide an extensive probabilistic characterization of the response process. However, it has turned out that this partial differential equation is in fact quite difficult to solve. A numerical approach will be provided in the next section to illustrate the evolution of probability density functions.

CHAPTER IV

NUMERICAL PROCEDURE

Path Integration Method

Over the years, large amount of effort has been directed to establish methods for solving the Fokker-Planck equation. However, exact solutions for the Fokker-Planck equations are known only for linear systems and for some very special first-order nonlinear systems. For most nonlinear systems, there is no general analytical method available to approximate solutions.

Instead of solving the Fokker-Planck equation directly to illustrate the evolution of probability density function, path integration method is a numerical solution technique used to handle these nonlinear problems. The transition and steady state probability density function corresponding to the Fokker-Planck equation can be obtained through a path integral solution procedure based on the assumption that the response vector can be approximated as jointly Gaussian. This assumption may be valid in the case of weak nonlinearities and when the excitation intensities are small.

If the Fokker-Planck equation is solved for the transition probability density, then the evolution of probability density $p(\vec{x},t)$ of $\vec{X}(t)$ can be obtained from (Lin et al 1997)

$$p(\vec{x},t)=\int_R q(\vec{x},t\mid\vec{x}^{(0)},t_0)\,p(\vec{x}^{(0)},t_0)d\vec{x}^{(0)} \tag{22}$$

where R is the range of the n-dimensional state space for $\vec{x}$ and $p(\vec{x}^{(0)},t_0)$ is the initial probability density of $\vec{X}(t)$ at $t = t_0$. By dividing the interval $[t_0, t]$ into N sub-intervals, a long term evolution of probability density over time can be computed in a series of shorter time steps as follows (Lin et al 1997).

$$p(\vec{x},t)=\int_R q(\vec{x},t)\,|\,\vec{x}^{(N-1)},t_{N-1})d\vec{x}^{(N-1)}\int_R q(\vec{x}^{(N-1)},t_{N-1}\,|\,\vec{x}^{(N-2)},t_{N-2})d\vec{x}^{(N-2)}$$
$$\cdots\int_R q(\vec{x}^{(2)},t_2\,|\,\vec{x}^{(1)},t_1)d\vec{x}^{(1)}\int_R q(\vec{x}^{(1)},t_1\,|\,\vec{x}^{(0)},t_0)\,p(\vec{x}^{(0)},t_0)d\vec{x}^{(0)} \qquad (23)$$

Therefore, the probability density function at the desired time for every point in state space can be evaluated by Equation (22) and (23) for the given initial probability density function.

The idea of numerical path integration is based on the fact that short term transition probability density can be approximated, and that long term evolution of probability density can be calculated from short term evolutions. It is necessary to obtain the short term transition probabilities, to select the proper time steps, and to evaluate the integrations in Equation (23) numerically. Each existing path integration method employs a certain interpolation scheme to integrate and represent the probability density by its values at discrete grid points. Also, different approaches are used for obtaining the short time transition probability as an approximate solution of the Fokker-Planck equation in short time steps.

In this project, the numerical procedure of path integration uses Equation (23) with the additional assumption that the transition probability density in each small time step is approximately Gaussian. This is based on the idea described in Lin et al (1997), where different forms of the short time transition probability density have been developed by solving moment equations to estimate the transition probability density function. The transition probability density multiplied with the probability density function of the previous time step is then integrated using a Gauss-Legendre interpolation scheme. Path integration method based on the Gauss-Legendre quadrature interpolation scheme is capable of producing accurate results of probability density as it evolves with time, including the tail region where the probability level is very low. This low probability region is important for the system reliability estimation

Gauss-Legendre Interpolation Scheme

The basis of the Gauss-Legendre interpolation scheme is equivalent to replacing the function to be integrated directly with an interpolation polynomial of a certain order. The values of the probability are obtained at the Gauss quadrature points in sub-intervals without explicit interpolation. The desired accuracy can be achieved with enough Gaussian points.

The derivation of this path integration method is straightforward. The expression of a typical step of probability evolution from t_{i-1} to t_i is as follows.

$$p(x^{(i)},t_i)=\int_{R_s} q(x^{(i)},t_i \mid x^{(i-1)},t_{i-1})\,p(x^{(i-1)},t_{i-1})dx^{(i-1)} \tag{24}$$

where R_s is the reduced range of the state space, usually an n-dimensional rectangle. The computation is carried out within a reduced finite range in the state space. It is provided that the probability evolution outside this range is sufficiently low and negligible. And $q(x^{(i)},t_i \mid x^{(i-1)},t_{i-1})$ is a conditional probability density, commonly known as the transition probability density.

The essential features of the Gauss-Legendre interpolation scheme are illustrated in a one-dimensional system for integral (24). The integral (24) is discretized into the composite Gauss-Legendre quadrature form (Lin et al 1997).

$$p(x^{(i)},t_i)=\sum_{k=1}^{K}\frac{\delta_k}{2}\sum_{l=1}^{L_k}c_{kl}\,p(x_{kl}^{(i-1)},t_{i-1})q(x^{(i)},t_i \mid x_{kl}^{(i-1)},t_{i-1}) \tag{25}$$

where K is the number of sub-intervals, L_k is the number of quadrature points in sub-interval k, δ_k is the length of sub-interval k, each x_{kl} is the position of a Gauss quadrature point, and c_{kl} is its corresponding weight. If the expression of the transition probability is known, Equation (25) can be used to calculate the probability density at any point $x^{(i)}$ at step i, provided that the probability density at the Gauss points are known at step i-1.

The positions of Gauss points and their weights can be found in standard textbooks on numerical analysis (e.g. Stroud 1974). For example, for two Gauss points in the interval (x_l, x_r), their positions and weights are

$$x_1 = x_l + 0.211375(x_r - x_l), \quad c_1 = 1$$
$$x_2 = x_r - 0.211375(x_r - x_l), \quad c_2 = 1$$

For three Gauss points in (x_l, x_r),

$$x_1 = x_l + 0.11270(x_r - x_l), \quad c_1 = 0.55556$$
$$x_2 = 0.5(x_r + x_l), \quad c_2 = 0.88889$$
$$x_3 = x_r - 0.11270(x_r - x_l), \quad c_3 = 0.55556$$

To proceed to step $i+1$, only the following probability density functions at the Gauss points are required.

$$p(x_{mn}^{(i)}, t_i) = \sum_{k=1}^{K} \frac{\delta_k}{2} \sum_{l=1}^{L_k} c_{kl}\, p(x_{kl}^{(i-1)}, t_{i-1}) q(x_{mn}^{(i)}, t_i \mid x_{kl}^{(i-1)}, t_{i-1}) \tag{26}$$

Equation (26) provides a scheme to calculate the evolution of the probability density function step by step, starting from a given initial probability density function. With the adoption of the Gauss-Legendre quadrature rule, the evolution of a continuous probability density function is approximated by stepwise evolutions at discrete Gauss points.

In order to perform stepwise computations using Equation (26), the value of transition probability $q(x_{mn}^{(i)}, t_i \mid x_{kl}^{(i-1)}, t_{i-1})$ for each Gauss point is needed.

Statistical Moment Equations

For a short time step, the transition probability can be accurately approximated as a Gaussian distribution. The Gaussian assumption is justified because it approaches exactly to a Gaussian distribution when time step approaches zero. However, even if Gaussian distribution is assumed, there are different approaches to determine the parameters.

Wehner & Wolfer (1983) and Naess & Moe (2000) derived the expression directly from the Itô differential equation. However, its use has several disadvantages. First, it is accurate only for a very small time step. The time steps must be kept very small, which increases the computation time. Secondly, when it is applied to the case of an oscillatory system, the resulting Gaussian distribution becomes a degenerated one, causing computational difficulties.

In this project, an alternative approach is used. Since each transition probability $q(x_{mn}^{(i)}, t_i \mid x_{kl}^{(i-1)}, t_{i-1})$ in Equation (26) is assumed to be Gaussian, it depends only on the conditional mean and variance of $X_{mn}(t_i)$. If this conditional mean and variance are determined, then the short time transition probability density can be constructed. That is to obtain the first and second moments using the moment equations. Then, the calculation described in Equation (26) is straightforward.

The equations of the statistical moments can be derived from the Fokker-Planck equation.

$$\frac{\partial q(\vec{x}, t \mid \vec{x}^{(0)}, t_0)}{\partial t} = -\frac{\partial}{\partial x_i}[\, f_i(\vec{x}, t) q(\vec{x}, t \mid \vec{x}^{(0)}, t_0)] + \frac{1}{2}\frac{\partial^2}{\partial x_i \partial x_j}[b_{ij}(\vec{x}, t) q(\vec{x}, t \mid \vec{x}^{(0)}, t_0)] \qquad (27)$$

If the generic polynomial function is considered (Francescutto & Naito 2004)

$$y(x) = x_1^{k_1} \cdot x_2^{k_2} \cdot \ldots \cdot x_n^{k_n}, \qquad \text{with } k_1 + k_2 + \ldots + k_n = k \qquad (28)$$

Then the statistical moment of order *k* can be calculated by evaluating the expectation value of the function *y(x)*, i.e.

$$E[y(x)] = \int_{-\infty}^{\infty} \ldots \int_{-\infty}^{\infty} y(x)\, p(x^{(0)}, t_0) q(x, t \mid x^{(0)}, t_0) dx dx_0 \qquad (29)$$

Finally, the evolutionary equation for the *k*-th order moment is as follows

$$\frac{d}{dt} E[y] = \sum_{i=1}^{n} E\left[f_i(x,t) \frac{\partial y}{\partial x_i} \right] + \frac{1}{2} \sum_{i,j=1}^{n} E\left[b_{ij}(x,t) \frac{\partial^2 y}{\partial x_i \partial x_j} \right] \qquad (30)$$

which can be further simplified by utilizing the linearity of the expectation operator.

The Gaussian Closure of Moments

In this project, the case of interest will focus on the ship rolling motion driven by colored noise process described by Equation (18). The procedure given in Equation (30) allows an easy computation for the evolutionary equations of the 4 first order and of the 10 second order moments of System (18). However, these moment equations constitute an infinite hierarchy in the case of nonlinear system. The 14 equations for the moments up to second order also include third and fourth order moments. When additional equations for the higher moments are derived, even higher moments are introduced. This is an infinite hierarchy form. In order to evaluate the higher order moments in terms of lower order, the closure of moments method is used.

In this project, since the short time transition probability density is approximately Gaussian, the infinite hierarchy may be truncated to second order. The simplest way to do would be just to neglect the third and fourth order moments but this is equivalent to neglect all the effect of nonlinearities. Therefore, the well-known Gaussian closure procedure is introduced. This approach is used to express higher order moments in terms of the first and second moments. The effect of the nonlinearities is explicitly taken into account although in an approximate way. So the transition probability density can be constructed in the Gaussian form to obtain values of $q(x_{mn}^{(i)}, t_i \mid x_{kl}^{(i-1)}, t_{i-1})$ at the Gauss points.

Gaussian closure is a technique for truncating the set of equations that result from consideration of a polynomial nonlinearity. For the scalar situation, the evolution of the *k*- th moment of *y(t)* can be written as follows (Lutes & Sarkani 2004).

$$\frac{1}{k}\frac{d}{dt}E[y^k(t)] + \sum_{j=0}^{J} a_k E[y^{j+k-1}(t)] = E[Q(t)y^{k-1}(t)] \tag{31}$$

Assuming that any moment of *y(t)* can be written in terms of mean and variance in the same way as for a Gaussian random variable, the higher order moment can be rewritten as follows (Lutes & Sarkani 2004)

$$E[y^m(t)] = \sum_{r=0,2,4}^{[m]} \frac{m!}{r!(m-r)!}(1)(3)\cdots(r-1)\mu_y^{m-r}(t)\sigma_y^r(t) \tag{32}$$

in which [*m*] denotes either *m* or *m*-1, depending on which is an even integer.

By using the Gaussian closure technique described above with the ship rolling motion system of interest, below is the 14 equations for the moments up to second order. (Su 2010)

$$\begin{aligned}
&\frac{d}{dt}E[x_1] = E[x_2] \\
&\frac{d}{dt}E[x_2] = -\mu E[x_2] - 3\delta E[x_2]E[x_2^2] + 2\delta E[x_2]^3 - E[x_1] - 3\alpha E[x_1]E[x_1^2] + \varepsilon E[x_4] \\
&\frac{d}{dt}E[x_3] = -c_1 E[x_3] - k_1^2 E[x_4] \\
&\frac{d}{dt}E[x_4] = E[x_3] \\
&\frac{d}{dt}E[x_1^2] = 2E[x_1x_2] \\
&\frac{d}{dt}E[x_2^2] = -2\mu E[x_2^2] - 6\delta E[x_2]^2 + 4\delta E[x_2]^4 - 2E[x_1x_2] - 6\alpha E[x_1^2]E[x_1x_2] \\
&\qquad\qquad + 4\alpha E[x_1]^3 E[x_2] + 2\varepsilon E[x_2x_4] \\
&\frac{d}{dt}E[x_3^2] = -2c_1 E[x_3^2] - 2k_1^2 E[x_3x_4] \\
&\frac{d}{dt}E[x_4^2] = 2E[x_3x_4] + \beta_1^2
\end{aligned} \tag{33}$$

$$
\begin{aligned}
\frac{d}{dt}E[x_1x_2] &= E[x_2^2]-\mu E[x_1x_2]-3\delta E[x_2^2]E[x_1x_2]+2\delta E[x_1]E[x_2]^3-E[x_1^2] \\
&\quad -3\alpha E[x_1]^2E[x_1^2]+2\alpha E[x_1]^4+\varepsilon E[x_1x_4] \\
\frac{d}{dt}E[x_1x_3] &= E[x_2x_3]-c_1E[x_1x_3]-k_1^2E[x_1x_4] \\
\frac{d}{dt}E[x_1x_4] &= E[x_2x_4]+E[x_1x_3] \\
\frac{d}{dt}E[x_2x_3] &= -\mu E[x_2x_3]-3\delta E[x_2^2]E[x_2x_3]+2\delta E[x_2]^3E[x_3]-E[x_1x_3] \\
&\quad -3\alpha E[x_1^2]E[x_1x_3]+2\alpha E[x_1]^3E[x_3]+\varepsilon E[x_3x_4]-c_1E[x_2x_3] \\
&\quad -k_1^2E[x_2x_4] \\
\frac{d}{dt}E[x_2x_4] &= -\mu E[x_2x_4]-3\delta E[x_2^2]E[x_2x_4]+2\delta E[x_2]^3E[x_4]-E[x_1x_4] \\
&\quad -3\alpha E[x_1^2]E[x_1x_4]+2\alpha E[x_1]^3E[x_4]+\varepsilon E[x_4^2]+E[x_2x_3] \\
\frac{d}{dt}E[x_3x_4] &= -c_1E[x_3x_4]-k_1^2E[x_4^2]+E[x_3^2]
\end{aligned}
\qquad (33)
$$

These moment equations are solved using the Gaussian closure technique to estimate the transition probability density function.

Transition Density Function

The transition probability density can be constructed in the Gaussian form to obtain values of $q(x_{mn}^{(i)}, t_i \mid x_{kl}^{(i-1)}, t_{i-1})$ at the Gauss points. This transition propagator $q(x_{mn}^{(i)}, t_i \mid x_{kl}^{(i-1)}, t_{i-1})$ is interpreted as the transition probability density function corresponding to the state x_{kl} at time $t_{i\text{-}1}$ passing to another state x_{mn} at time t_i

In the one-dimensional case, assume that the closed moment equations for the mean and mean square are in the following forms (Lin et al 1997)

$$\begin{aligned} \dot{m}_1 &= h_1(m_1, m_2, t) \\ \dot{m}_2 &= h_2(m_1, m_2, t) \end{aligned} \tag{34}$$

where $m_1 = E[X]$, $m_2 = E[X^2]$, and E denotes an ensemble average. Since the state of the system at the previous time step is assumed to be known, namely, $X = x_{kl}^{(i-1)}$, $t = t_{i\text{-}1}$, Equation (34) are solved for the following step $t_i = t_{i-1} + \Delta t_i$ with the initial conditions

$$m_1(t_{i-1}) = x_{kl}^{(i-1)}, \;\; m_2(t_{i-1}) = [x_{kl}^{(i-1)}]^2 \tag{35}$$

The short time transition probability density from $x_{kl}^{(i-1)}$ at $t_{i\text{-}1}$ to x_{mn}^{i} at t_i can be approximated as

$$q(x_{mn}^{(i)}, t_i \mid x_{kl}^{(i-1)}, t_{i-1}) = \frac{1}{\sqrt{2\pi}\sigma(t_i)} \exp\left\{ -\frac{[x_{mn}^{(i)} - m_1(t_i)]^2}{2\sigma^2(t_i)} \right\} \tag{36}$$

where $\sigma^2(t_i) = m_2(t_i) - [m_1(t_1)]^2$. Using Equation (36), the short time transition probability density $q(x_{mn}^{(i)}, t_i \mid x_{kl}^{(i-1)}, t_{i-1})$ at the Gauss points can be evaluated. Within a short time interval, the transition probability density has significant value only in the neighborhood of the starting point $x_{kl}^{(i-1)}$. Therefore, for each starting point, only a few destination Gauss points need to be taken into consideration. The transition probabilities at other Gauss points may be neglected. This can be implemented by saving only the results of those destination points for which the transition probabilities cannot be ignored.

For time-invariant systems, Equations (34) are time independent. Then the use of constant time steps is convenient. It is convenient to divide the time range into N equal steps $\Delta t = (t\text{-}t_0)/N$ since the transition probability $q(x_{mn}^{(i)}, t_i \mid x_{kl}^{(i-1)}, t_{i-1})$ remains unchanged for each time step. The values $q(x_{mn}^{(i)}, t_i \mid x_{kl}^{(i-1)}, t_{i-1})$ at all Gaussian points need to be calculated only once. They can be stored for repeated use in all subsequent steps.If the system is not time-invariant, then the short time transition probability densities $q(x_{mn}^{(i)}, t_i \mid x_{kl}^{(i-1)}, t_{i-1})$ must be recomputed for each time step. This is time-consuming. Re-

evaluating the transition probability at each step can consume more than 95% of the total computation time.

A special case of time-variant system is one in which the drift coefficients or diffusion coefficients or both in Itô stochastic differential equations (19) and (20) are time-variant but have a common period. In this case, we need only to calculate transition probabilities $q(x_{mn}^{(i)}, t_i \mid x_{kl}^{(i-1)}, t_{i-1})$ for a certain number of time steps for the first period and then store the results for all subsequent periods.

Assuming the initial probability density function obeys the Gaussian distribution, Equation (26) provides a scheme by the path integration method to calculate the evolution of a probability density step by step, starting from a given initial probability density. The probability densities at desired time will be calculated from Equation (26) with transition probability given by equation (36) and the initial probability density.

In the next section, the numerical path integration procedure will be applied to a one-dimensional nonlinear system and a two-dimensional Duffing oscillator system in order to verify the written program following the described approach above.

Examples

Two examples with known exact transient or exact stationary solutions are given to illustrate the performance and capabilities of the numerical procedure of the path integration method described above. The numerical results agree very well with the exact solutions.

As the first example, consider a one-dimensional nonlinear system

$$\dot{X} - \alpha X + \beta X^3 = \sigma N(t), \quad (\alpha, \beta, \sigma > 0) \tag{37}$$

where *N(t)* is a unit Gaussian white noise. This system has an exact stationary probability density with two peaks

$$p_s(x) = C \exp\left[\frac{1}{2\sigma^2}(2\alpha x^2 - \beta x^4)\right] \tag{38}$$

where C is the normalization coefficient. Equation (37) can be written in the form of Itô stochastic equation (19) as

$$dX(t) = (\alpha X - \beta X^3)dt + \sigma dW(t) \tag{39}$$

leading to the following Fokker-Planck equation according to equation (21)

$$\frac{\partial q}{\partial t} = -\frac{\partial(\alpha X - \beta X^3)q}{\partial X} + \frac{\sigma^2}{2}\frac{\partial^2 q}{\partial X^2} \tag{40}$$

Then, moment equations can be derived from the Fokker-Planck equation. Using Gaussian closure, the first two moment equations are obtained as

$$\begin{aligned} \frac{d}{dt}E[X] &= \alpha E[X] - 3\beta E[X]E[X^2] + 2\beta E[X]^3 \\ \frac{d}{dt}E[X^2] &= 2\alpha E[X^2] - 6\beta E[X^2]^2 + 4\beta E[X]^4 + \sigma^2 \end{aligned} \tag{41}$$

Equation (41) can be solved numerically. The moments obtained are used to form the approximate Gaussian transition probability given by equation (36).

In numerical computation, the system parameters chosen for this example are α = 0.5, β = 0.5 and σ = 0.5, and a time step Δt = 0.1. The initial probability density is given by equation (42)

$$p(x^{(0)},0) = \frac{1}{\sqrt{2\pi}\eta}\exp\left[-\frac{(x^{(0)}-\mu)^2}{2\eta^2}\right] \tag{42}$$

with μ = -2.0 and η = 0.2. The reduced range for path integration is chosen to be [-3, 3]. It is divided into 30 uniform sub-intervals with two quadrature points in each sub-interval. That is K = 30, δ_k = 6/30, and L_k = 2 in equation (26). The system response probability density is evolved, starting from the initial probability density given by equation (42).

After 100 steps or t = 10, the computed probability density is nearly stationary. After t = 100, the computed probability density function was observed long enough for

convergence to the stationary solution. The computed probability density at t = 100 is shown in a linear scale in Figure 6. and in a logarithmic in Figure 7. The exact solutions are also included in the figure for comparison. It is seen that the numerical scheme yields accurate results even at very low probability levels.

The second example selected for illustration is the following Duffing oscillator subjected to a unit white noise excitation

$$\ddot{X} + 2\beta\dot{X} + \xi X + \lambda X^3 = \sigma N(t) \tag{43}$$

where *N(t)* is again assumed to be a unit Gaussian white noise. This system has an exact stationary joint probability density function of displacement and velocity

$$p_s(x,\dot{x}) = C\exp\left\{-\frac{2\beta}{\sigma^2}\left(\dot{x}^2 + \xi x^2 + \frac{\lambda}{2}x^4\right)\right\} \tag{44}$$

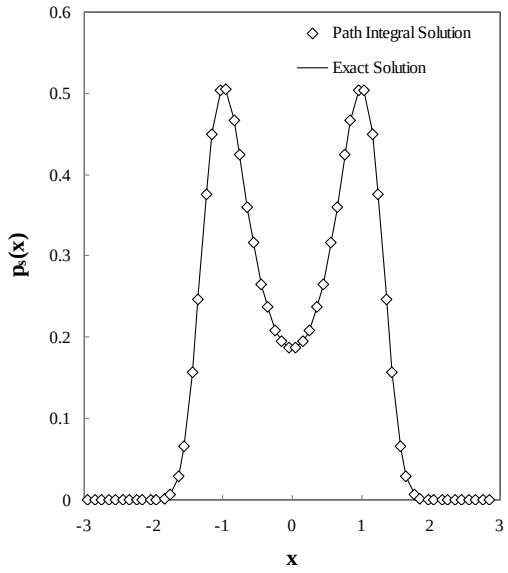

Figure 6. Stationary probability densities for system (37) in linear scale

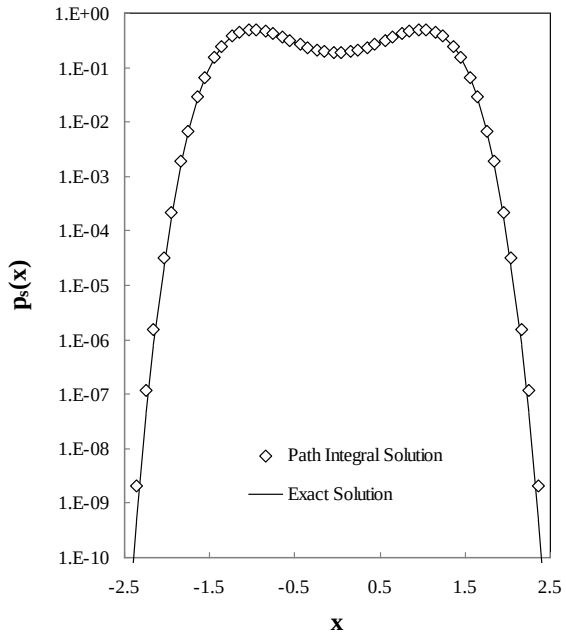

Figure 7. Stationary probability densities for system (37) in logarithmic scale

Introducing $X_1 = X$ and $X_2 = \dot{X}$, equation (3.23) can be written in the form of Itô stochastic equation (2.19) as

$$\begin{pmatrix} dX_1(t) \\ dX_2(t) \end{pmatrix} = \begin{pmatrix} X_2 \\ -2\beta X_2 - \xi X_1 - \lambda X_1^3 \end{pmatrix} dt + \begin{pmatrix} 0 \\ \sigma \end{pmatrix} d\vec{W}(t) \tag{45}$$

and the corresponding Fokker-Planck equation is

$$\frac{\partial q}{\partial t} = \frac{\partial (2\beta X_2 + \xi X_1 + \lambda X_1^3) q}{\partial X_2} - X_2 \frac{\partial q}{\partial X_1} + \frac{\sigma^2}{2} \frac{\partial^2 q}{\partial X_2^2} \tag{46}$$

The equations for the first and second order moments on the basis of Gaussian closure are given by

$$
\left.
\begin{aligned}
&\frac{d}{dt}E[X_1] = E[X_2] \\
&\frac{d}{dt}E[X_2] = -2\beta E[X_2] - \xi E[X_1] - 3\lambda E[X_1]E[X_1^2] + 2\lambda E[X_1]^3 \\
&\frac{d}{dt}E[X_1^2] = 2E[X_1X_2] \\
&\frac{d}{dt}E[X_1X_2] = E[X_2^2] - 2\beta E[X_1X_2] - \xi E[X_1^2] - 3\lambda E[X_1^2]^2 + 2\lambda E[X_1]^4 \\
&\frac{d}{dt}E[X_2^2] = -4\beta E[X_2^2] - 2\xi E[X_1X_2] - 6\lambda E[X_1^2]E[X_1X_2] + 4\lambda E[X_1]^3 E[X_2]
\end{aligned}
\right\} \quad (47)
$$

These equations were then solved numerically for a short time step Δt. The moments obtained were used to form the two-dimensional Gaussian transition probability density.

The initial distribution was assumed to be Gaussian with a two-dimensional probability density

$$p(x^{(0)}, \dot{x}^{(0)}) = \frac{1}{2\pi s_1 s_2} \exp\left\{ -\frac{(x^{(0)} - \mu_1)^2}{2s_1^2} - \frac{(\dot{x}^{(0)} - \mu_2)^2}{2s_2^2} \right\} \quad (48)$$

where μ_1 = -2.0, μ_2 = -1.8, s_1 = 0.1 and s_2 = 0.1. The evolution of the probability density with the system parameters ξ = 1.0, λ = 0.2, β = 0.2, and σ^2 = 0.1 was computed with a time step of Δt = 0.4. A reduced state space is within [-3, 3] x [-3, 3]. It is divided into 30 uniform sub-intervals in each direction with two quadrature points in each sub-interval. That is K = 30, δ_k = 6/30, and L_k = 2 in equation (25).

The marginal stationary probability densities of X and $\dot{X}$ are shown in Figure 8. and Figure 9., respectively. Both are seen to be accurate even at extremely low probability levels.

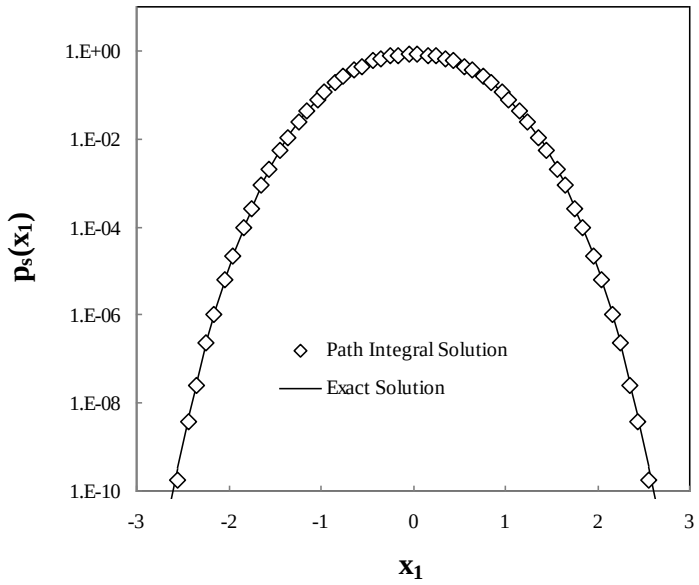

Figure 8. Probability density of X_1

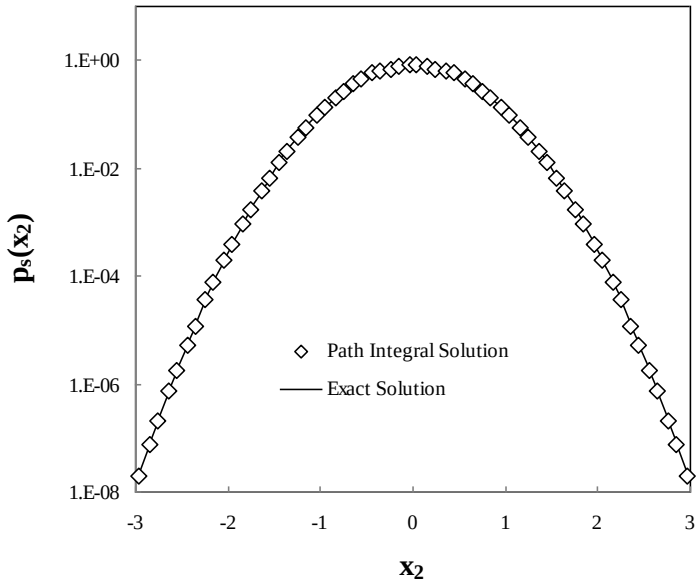

Figure 9. Probability density of X_2

In next chapter, the procedure discussed above will be applied to ship rolling motion problem to illustrate the difference in system response when the vessel is subjected to various types of excitation.

CHAPTER V

RESULTS

Ship Description

In this project, the nonlinear near-capsizing behavior of a ship in both regular and random seaway is analyzed. The vessel considered is an ocean surveillance ship T-AGOS. The ship's hull design prevents the vessel from rolling in the heavy seas. The value of the metacentric height (GM) for the T-AGOS is 3.618 m (11.871 ft) with a corresponding angle of vanishing stability of ± 68.8º. Figure 10. shows the corresponding GZ curve.

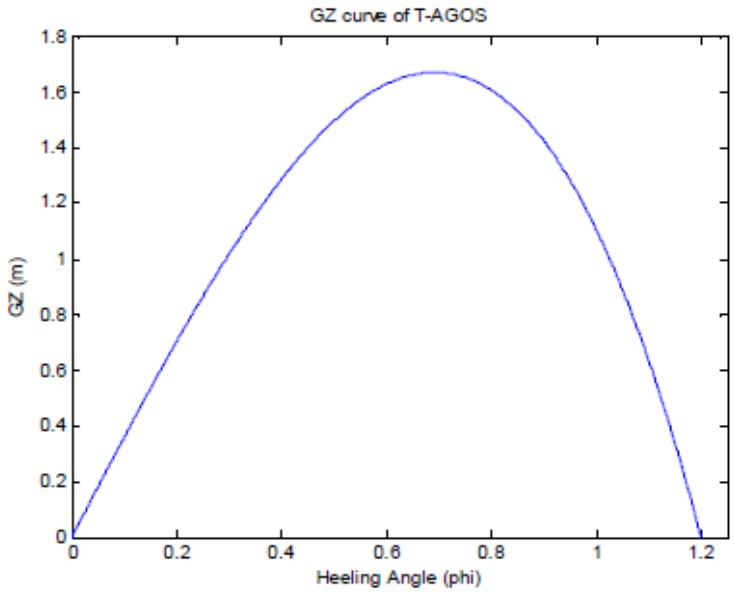

Figure 10. GZ curve of T-AGOS (Mulk & Falzarano 1994)

Ship Rolling System

Firstly, the ship rolling motion in the unforced (F_{sea} = 0) and undamped (B_{44} = B_{44q} = 0) system is considered. This system is referred to as the unperturbed system. It will be used for evaluating the effects of damping and wave excitation later.

$$(I_{44} + A_{44}(\omega))\phi'' + \Delta(C_1\phi - C_3\phi^3) = 0 \tag{49}$$

Equation (5.1) can be rewritten in the following nondimensional form

$$\ddot{x}(t) + x(t) - \alpha x^3(t) = 0 \tag{50}$$

Phase portrait of equation (50) is shown in Figure 11. A typical ship with or without a loll angle will have positive and negative angles of vanishing stability. These angles of vanishing stability are also shown in phase portrait. They are connected to one another by a heteroclinic connection shown in Figure 11. This special curve is called a separatrix. Initial conditions inside these connections result in bounded rolling oscillations while initial conditions outside result in unbounded oscillations or capsizing.

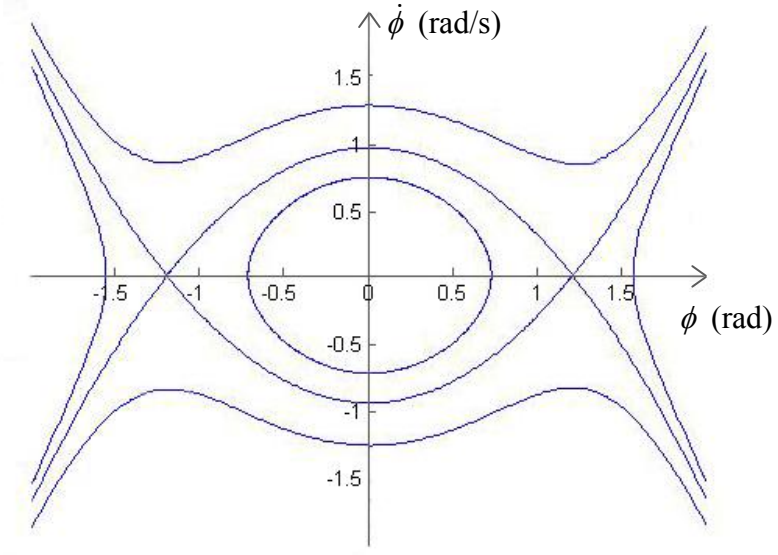

Figure 11. Phase portrait of the unperturbed system

If damping is included in the model as in equation (51)

$$\ddot{x}(t) + \mu\dot{x}(t) + \delta\dot{x}^3(t) + x(t) - \alpha x^3(t) = 0 \tag{51}$$

then the system is not conservative. These trajectories are still invariant with respect to time but the heteroclinic connections split as shown in Figure 12. The coefficients of linear and nonlinear damping terms are set as constant by assuming a fixed frequency. The parameters correspond to equation (51) are as following: μ = 0.1321, δ = 0.02656, α = -0.9018

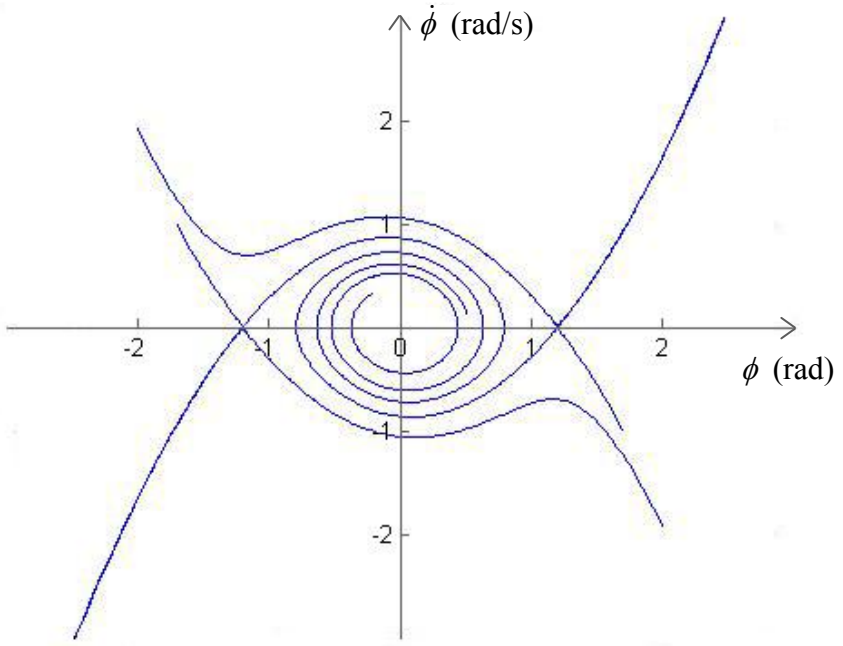

Figure 12. Phase portrait with heteroclinic connection split

The separatrix of the undamped system is replaced by invariant manifolds. The stable manifold originates from infinity and approaches the saddle point at angle of vanishing stability. Another one is the unstable manifold. It originates at the saddle and approaches the stable node at the origin.

When time dependence is added to the differential equation of motion through forcing as in equation (52), the trajectories are not invariant with respect to time. If the time dependence is period, the time dependence may be eliminated by the use of Poincaré map.

$$\ddot{x}(t) + \mu\dot{x}(t) + \delta\dot{x}^3(t) + x(t) - \alpha x^3(t) = A\cos\omega t \tag{52}$$

In order to specify an initial condition, the roll angle, the roll velocity, and the forcing phase must be known. Because of the additional wave excitation, the system becomes a three-dimensional extended phase space. This three-dimensional extended phase space can be reduced to two dimensions by making use of the Poincaré map. That is to sampling the roll angle and the roll velocity at integer multiples of the excitation period. In our case, the wave frequency is ω = 0.97 rad/s. In this way, the period motions are represented by fixed points of the map. The stable and unstable manifolds described above are two-dimensional sets in the extended phase space while their representations in terms of the map are one-dimensional curves. The Poincaré maps are constructed. Figure 13. shows an example of a deterministic roll motion represented by the Poincaré map. By using different time instant for constructing the Poincaré map, we are able to capture different Poincaré map as shown in Figure 14.

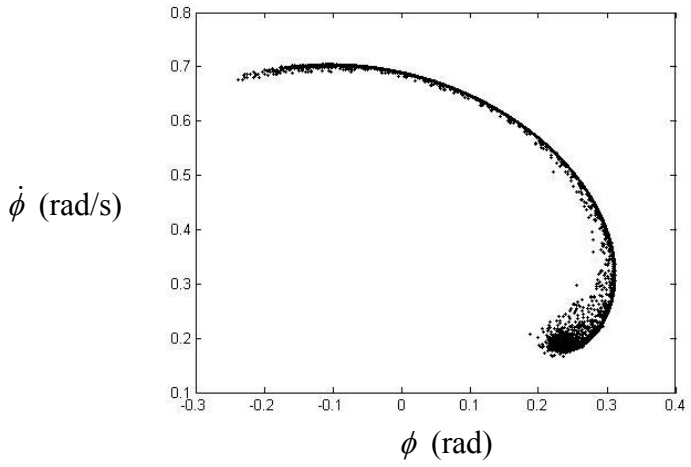

Figure 13. The Poincaré map at every period for periodic excitation

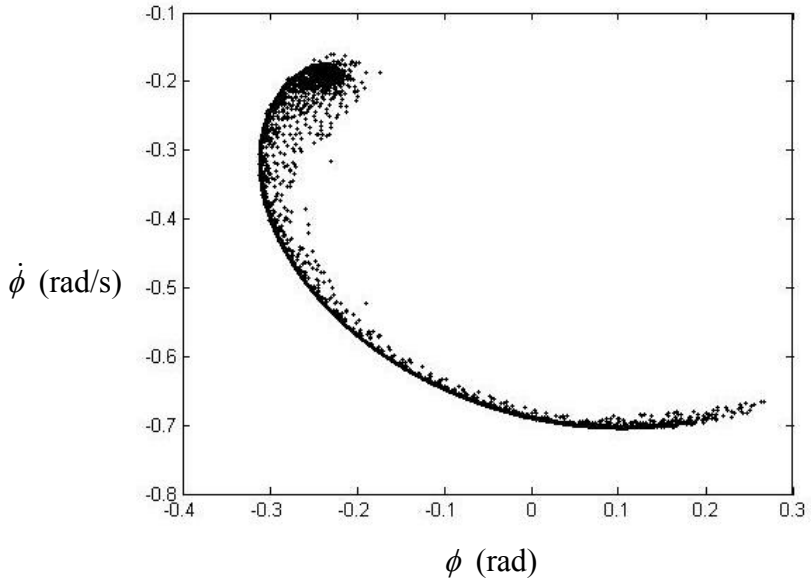

Figure 14. The Poincaré map at every 1.5 period for periodic excitation

Practically, long trains of pure regular waves do not exist. The work mentioned above using regular beam waves as a simplified sea state. But realistic waves are random and irregular waves. To take into account the presence of randomness in the excitation and the response, a more realistic work is using random beam sea in single-degree-of-freedom roll model. The perturbed waveforms may be modeled as regular waves with Gaussian white noise as the external disturbance as in equation (53). With noise intensity, the response appears random as shown in Figure 15.

$$\ddot{x}(t) + \mu\dot{x}(t) + \delta\dot{x}^3(t) + x(t) - \alpha x^3(t) = A\cos\omega t + \sqrt{D}N(t) \tag{53}$$

Under random sea waves, one must deal with probabilistic approaches when studying stochastic stability, response, and reliability of ship roll motion. The evolution of the probability density function is another way to describe the behavior of the nonlinear roll motion in random waves. The behavior of the noisy forced ship roll motion under periodic excitation with Gaussian white noise can be modeled as a Markov process. The probability density function of a Markov process satisfies a deterministic partial differential equation called the Fokker-Planck equation. The associated Fokker-

Planck equation governing the evolution of the probability density function of the roll motion is derived and numerically solved by the path integral method based on Gauss-Legendre interpolation to obtain joint probability density functions in state space.

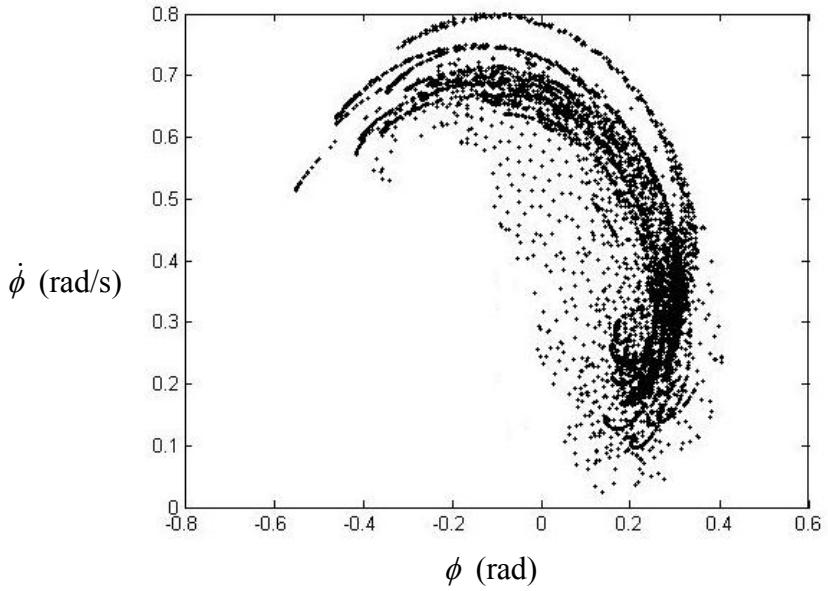

Figure 15. The Poincaré map with higher noise intensity

In the presence of a small random disturbance to the external period excitation, the imprint of the Poincaré map is preserved and can be identified via the joint probability density function on the Poincaré section as shown in Figures 16, 18 and 20. The probability density function indicates the preferred locations of the trajectories in the average sense.

The contour plots of the joint probability density function and their marginal probability density functions are shown in Figures 16 - 21. It is seen that the value of joint probability density decreases gradually as time progresses. For example, in Figure 18, the maximum value of joint probability density is about 0.5 when t = 12.95 s, and it is about 0.0011 when t = 74.45 s. Moreover, for the high intensity of white noise, the value of joint probability density decreases more quickly as time progresses. For

example, when t = 29.13 s, the maximum value of joint probability density is about 0.34 in Figure 16, it is about 0.12 in Figure 18, and it is only about 0.002 in Figure 20. These conclusions are farther demonstrated by the marginal probability density function in Figures 17, 19 and 21.

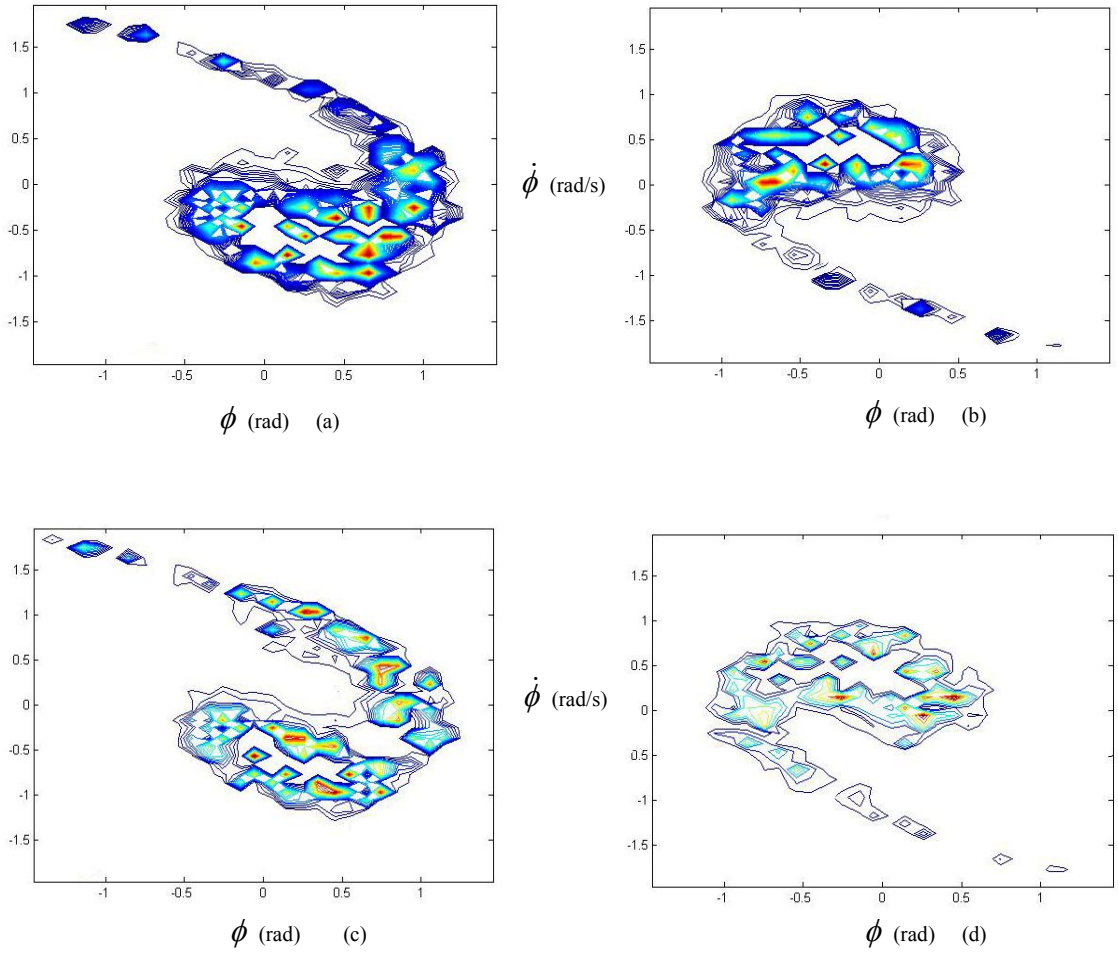

Figure 16. Evolution of contour plot of the joint probability density function with (*H, D, ω*) = (0.3, 0.01, 0.97) at time (a) *t* = 12.95 s (b) *t* = 29.13 s (c) *t* =45.32 s (d) *t* = 74.45 s

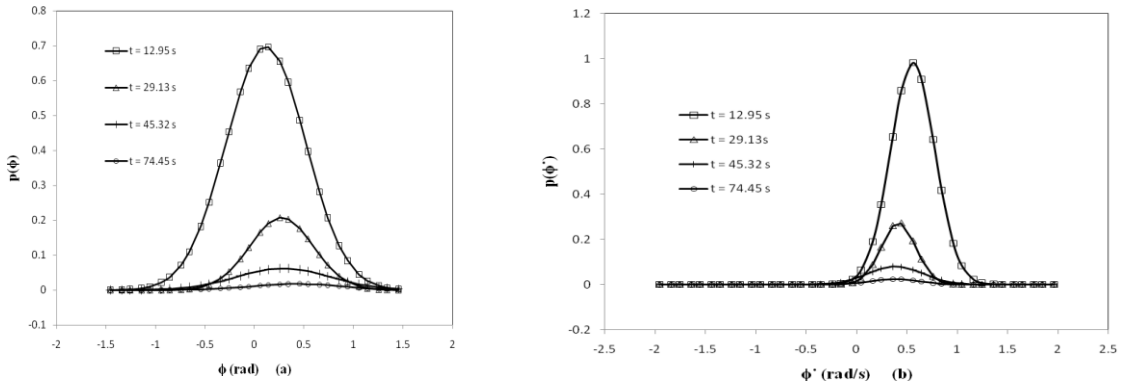

Figure 17. Marginal probability density function with (*H, D, ω*) = (0.1, 0.01, 0.97) (a) of roll angle; (b) of roll angular velocity

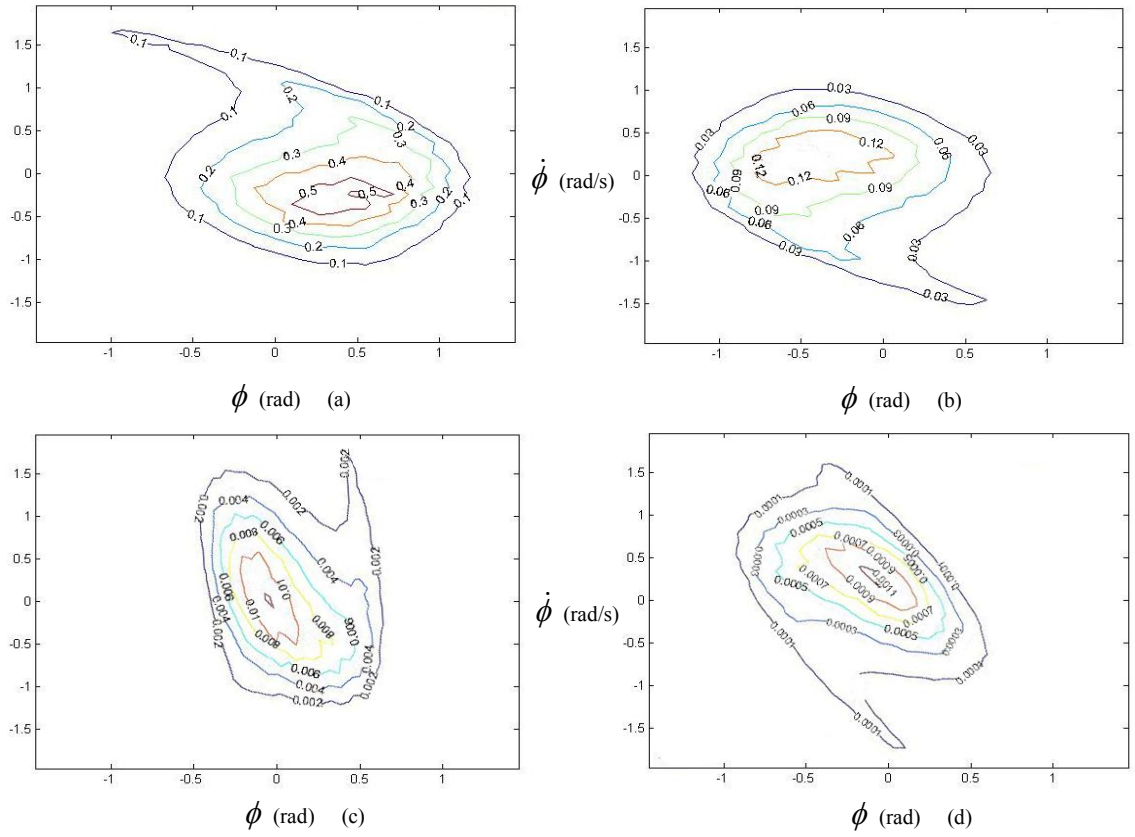

Figure 18. Evolution of contour plot of the joint probability density function with (*H, D, ω*) = (0.3, 0.05, 0.97) at time (a) *t* = 12.95 s (b) *t* = 29.13 s (c) *t* =45.32 s (d) *t* = 74.45 s

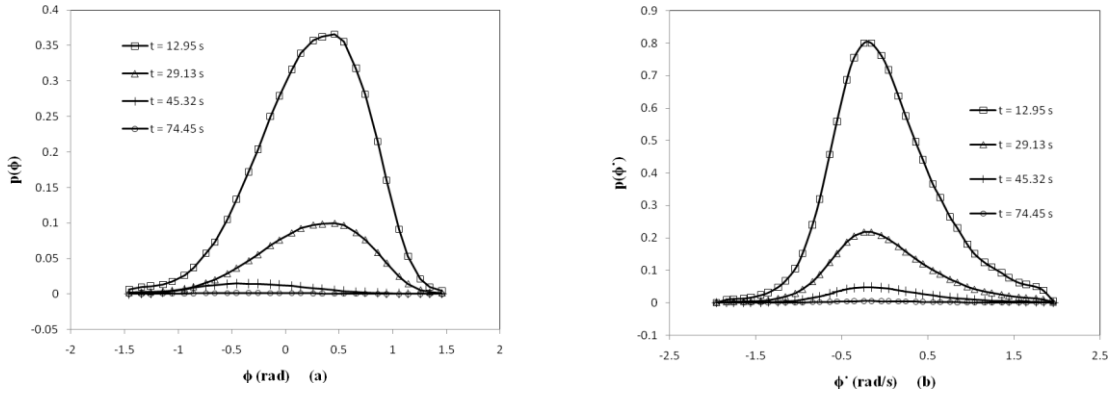

Figure 19. Marginal probability density function with (*H, D, ω*) = (0.3, 0.05, 0.97) (a) of roll angle; (b) of roll angular velocity

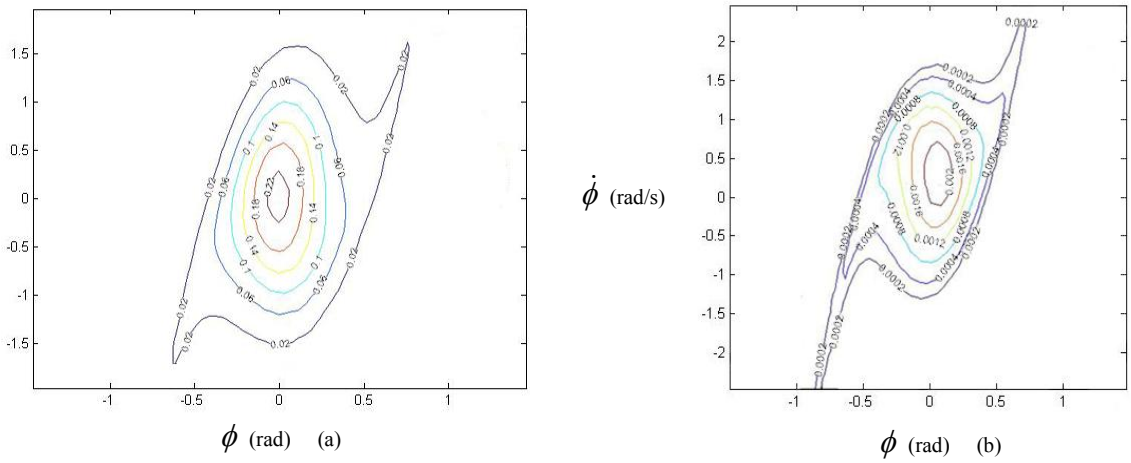

Figure 20. Evolution of contour plot of the joint probability density function with (*H, D, ω*) = (0.3, 0.1, 0.97) at time (a) *t* = 12.95 s (b) *t* = 29.13 s

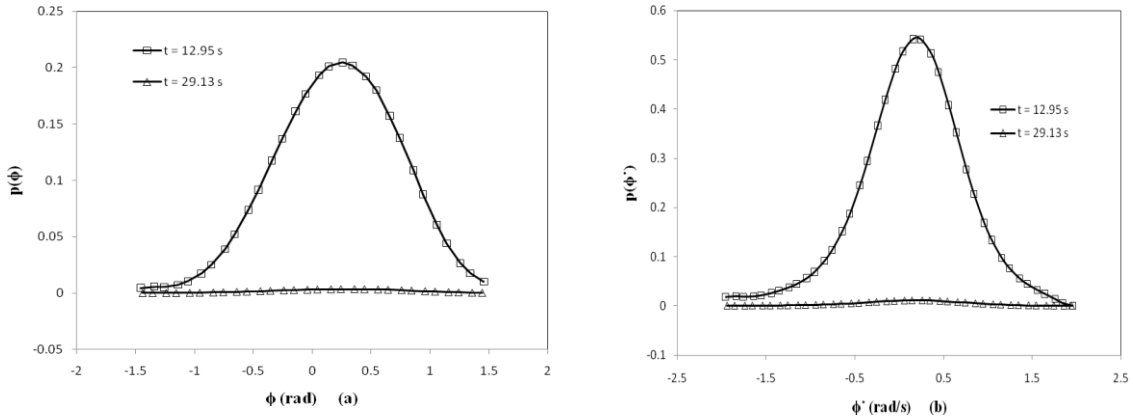

Figure 21. Marginal probability density function with (*H, D, ω*) = (0.3, 0.1, 0.97) (a) of roll angle; (b) of roll angular velocity

By defining the state domain surrounded by the two heteroclinic connections of Figure 11. as the safe domain, the probability of ship rolling restricted within the safe domain excited by above three sets of wave parameters are shown in Figure 22.

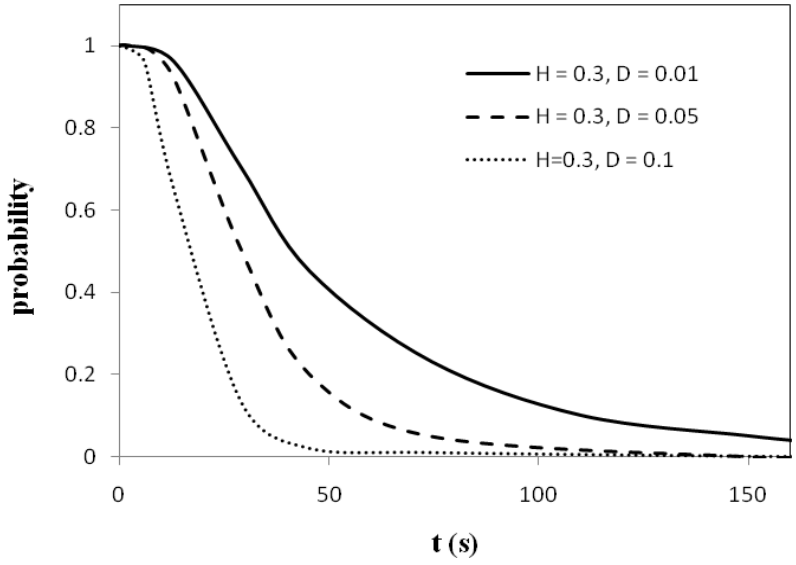

Figure 22. Probability of the ship rolling within the safe domain when ω = 0.97 rad/s

The time-dependent probability of ship rolling restricted within the safe domain is provided in Figure 22. It is found that the probability decreases as time progresses and it decreases much more quickly for the high intensity of the white noise. At t = 45.32 s, the probability is about 45% when D = 0.01 It is about 20% when D = 0.05, and it is only about 2% when D = 0.1. The ship will finally leave the safe domain and capsize in the probability's view.

To further study the qualitative behavior of the ship roll motion and capsize of ships in probability space, the wave excitation is treated as colored noise. When the excitations are not white, it is quite useful to introduce the so-called filter equations. They represent the equations of motion of ideal systems excited by a white noise process input and finally give as response the particular nonwhite excitations considered. If these equations are added to the original equations of motion, the whole system can be considered as excited by a white noise process. The output of the filter is used to drive the nonlinear system.

In this project, the primary goal is to show the possibilities of using path integration for systems where the noise is filtered, increasing the dimensionality of the problem to four. The method is based on the assumption that the input excitation can be obtained by filtering white noise processes. In this way the advantage of considering the input as a white noise process is still obtained. It is then possible to model the response of nonlinear systems subjected to white noise or filtered white nosie in terms of a Markov vector process. The transitional probability density function is governed by the Fokker-Planck equation.

Equation (54) shows the ship rolling equation of motion with linear filtered white noise.

$$\begin{aligned} &\ddot{x}(t)+\mu\dot{x}(t)+\delta\dot{x}^3(t)+x(t)-\alpha x^3(t)=\varepsilon f(t) \\ &\ddot{f}(t)+c_1\dot{f}(t)+k_1^2 f(t)=\beta_1\dot{N}(t) \end{aligned} \tag{54}$$

The Poincaré map in Figure 23. is constructed using the sum of a set of harmonic wave excitation moment as an input excitation.

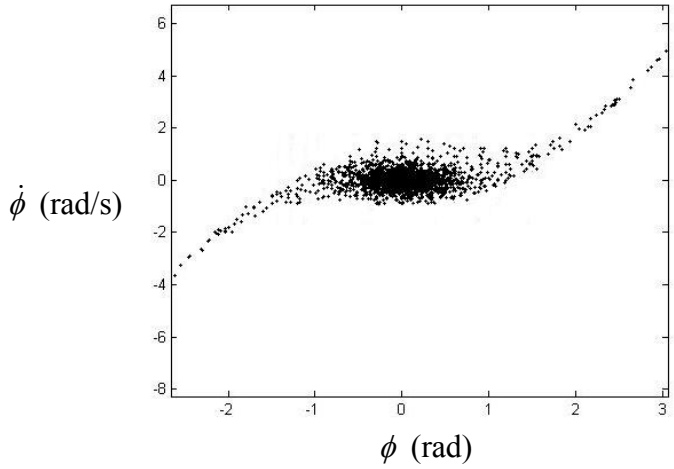

Figure 23. The Poincaré map using the sum of a set of harmonic wave excitation

As described above, the imprint of the Poincaré map is preserved and can be identified via the joint probability density function on the Poincaré section. The Poincaré map in Figure 23. is used to verify the joint probability density function obtained from the colored noise method in Figure 24.

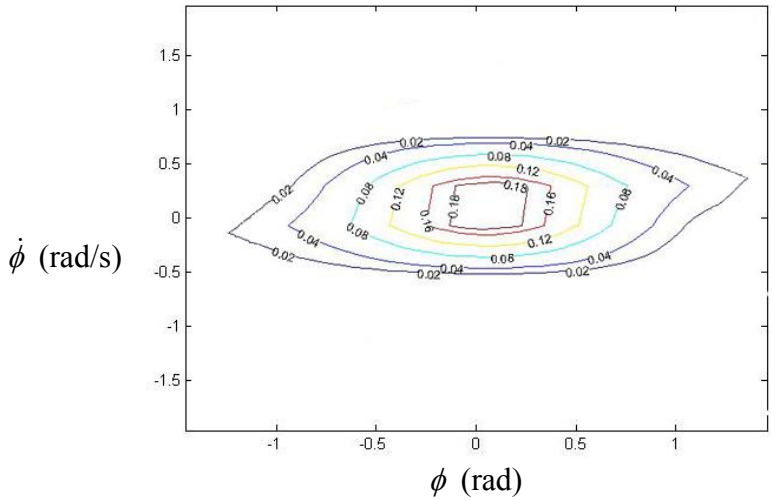

Figure 24. Contour of joint probability density function corresponding to 6 m wave height

It is shown that Figure 24. also follows the hypothesis about the imprint of the Poincaré map and the joint probability density function. We also recognize that contour plots of joint probability density function in the case of perturbed excitation with high noise intensity in Figure 20. and in the case of colored noise in Figure 24. look similar.

However, path integration method using a Gauss-Legendre interpolation scheme is not a good application for this study. The case of colored noise could not be further studied since high and low order moments' values will be of very different scales. The resulting ordinary differential equation system will be almost singular matrix. Solving the ordinary differential equations numerically requires a time-stepping method that is stable over a large range of time scales. But the moment equations easily become numerically unstable as the parameter connecting lower and higher order moments are in very different scales.

CHAPTER VI

CONCLUSION

Conclusion

This project represents an attempt to study the qualitative behavior of the ship roll motion in probability space. The stochastic nonlinear dynamic behaviors and the probability density function of ship rolling in the random beam wave are studied. The probability density function for the response of the system is obtained numerically for all excitation types and with varying amount of noise.

In this project, we have pursued a study of the response of a nonlinear system excited by a harmonic motion with additive white noise first. The probability density function of rolling response is evaluated and the time-dependent probability of ship rolling restricted within the safe domain is provided. It is found that the value of joint probability density decreases gradually as time progresses. And it decreases much more quickly for the high intensity of white noise. The ship will leave the safe domain for enough time and capsize in the probability's view.

Then, a nonlinear study of ship rolling in a stochastic beam sea represented by colored noise as the Pierson-Moskowitz spectrum has been conducted. Even the path integration method based on Gauss-Legendre interpolation scheme is not a good application to ship rolling motion with high dimensionality, a preliminary result still shows the effect of colored noise to the ship rolling motion.

Future Work

Since the evolution of joint probability density function can be used to explain the global behavior of the ship rolling motion, the path integration method with different interpolation scheme should be further studied. The procedure developed by Naess and Moe [2000] is an alternative one. It uses a time discretization scheme where the noise

has a known distribution and only appear in one variable of discretized system of one-dimension stochastic differential equations. This requires shorter time steps and an efficient and accurate interpolation method.

Moreover, it is well-known that for large roll motions, the effect of coupling among roll, heave and sway motions may not be negligible. This would require non-trivial advances in ship modeling. Also, in all cases discussed in this project, the system models excitation arising from beam seas. The results for motions in quartering and heading seas should also be obtainable, since these effects generally introduce combined parametric and external excitation.

REFERENCES

Davies, H. G., Liu, Q. 1990 The response envelope probability density function of a Duffing oscillator with random narrow-band excitation. Journal of Sound and Vibration, **139**.

Davies, H. G., Nandall, D. 1986 Phase plane for narrow band random excitation of a Duffing oscillator. Journal of Sound and Vibration, **104**.

Falzarano, J. M., Shaw, S. W., Troesch, A. W. 1992 Application of global methods for analyzing dynamical systems to ship rolling motion and capsizing. International Journal of Bifurcation and Chaos, **2**.

Francescutto, A., Naito, S. 2004 Large amplitude rolling in a realistic sea. Internation Shipbuilding Progess, **51**.

Hsieh, S. R., Troesch, A. W., Shaw, S. W. 1994 A nonlinear probabilistic method for predicting vessel capsizing in random beam seas. Proceedings of the Royal Society of London, **446**.

Hu, K., Ding, Y., Wang, H., Li, J. 2010 Application of the random melnikov method for single-degree-of-freedom vessel rolls motion. Proceedings of OMAE 2010.

Huang, Z. L., Zhu, W. Q., Ni, Y. Q., Ko, J. M. 2002 Stochastic averaging of strongly non-linear oscillators under bounded noise excitation. Journal of Sound and Vibration, **254**.

Lin, H., Yim, S. C. S. 1995 Chaotic roll motion and capsize of ships under periodic excitation with random noise. Applied Ocean Research, **17**.

Lin, H., Yim, S. C. S. 2001 Unified analysis of complex nonlinear motions via densities. Nonlinear Dynamics, **24**.

Lin, Y. K., Yu, J. S., Cai, G. Q. 1997 A new path integration procedure based on Gauss-Legendre scheme. Non-Linear Mechanics, **32**.

Liqin, L., Yougang, T. 2007 Stability of ships with water on deck in random beam waves. Journal of Vibration and Control, **13**.

Lutes, L. D., Sarkani, S. 2004 Random vibrations: analysis of structural and mechanical systems. Elsevier.

McCue, L., Wu, W. 2008 Application of the extended Melnikov's method for single-degree-of-freedom vessel roll motion. Ocean Engineering, **35**.

Mulk, T. U., Falzarano, J. M. 1994 Large amplitude rolling motion of an ocean survey vessel. SNAME Journal of Marine Technology.

Naess, A., Moe, V. 2000 Efficient path integration methods for nonlinear dynamic systems. Probabilistic Engineering Mechanics, **15**.

Naess, A., Moe, V. 2008 A numerical study of the existence and stability of some chaotic attractors by path integration. Journal of Vibroengineering, **10**.

Roberts, J. B., Vasta, M. 2000 Markov modeling and stochastic identification for nonlinear ship rolling in random waves. Philosophical Transactions: Mathematical, Physical and Engineering Sciences, **358**.

Stroud, A. H. 1974 Numerical quadrature and solution of ordinary differential equations. Springer, New York.

Su, Z. 2010 Rolling motion stability analysis in random sea by Gaussian and non-Gaussian moment closure methods. Dissertation Progressing Report.

Wehner, M. F., Wolfer, W. G. 1983 Numerical evaluation of path-integral solutions to Fokker-Planck equations. Physical Review A, **27**.

Xie, W. X., Cai, L., Xu, W. 2007 Numerical simulation for a Duffing oscillator driven by colored noise using nonstandard difference scheme. Physica A: Statistical and Theoretical Physics, **373**.

VITA

Name:	Arada Jamnongpipatkul
Address:	CE/TTI, Fl.8, Mailbox 105, 3136 TAMU, College Station, TX 77843
Email Address:	ajamnong@yahoo.com
Education:	B.Eng., Civil Engineering, Chulalongkorn University, 2008 M.S., Ocean Engineering, Texas A&M University, 2010